Exploring a COVID-19 Endemic Scenario: High-Resolution Agent-Based Modeling of Multiple Variants

(Article begins on next page)

15 May 2024

Exploring a COVID-19 endemic scenario: high-resolution agent-based modeling of multiple variants

Agnieszka Truszkowska, Lorenzo Zino, Sachit Butail, Emanuele Caroppo, Zhong-Ping Jiang, Alessandro Rizzo, Maurizio Porfiri*

Dr. A. Truszkowska

Center for Urban Science and Progress, Tandon School of Engineering, New York University, 370 Jay Street, Brooklyn, NY 11201, U.S.

Department of Mechanical and Aerospace Engineering, Tandon School of Engineering, New York University, Six MetroTech Center, Brooklyn NY 11201, U.S.

Department of Chemical and Materials Engineering, University of Alabama in Huntsville, 301 Sparkman Drive, Huntsville AL 35899, U.S.

Dr. L. Zino

Engineering and Technology Institute Groningen, University of Groningen, Nijenborgh 4, 9747 AG Groningen, The Netherlands

Department of Electronics and Telecommunications, Politecnico di Torino, 10129 Turin, Italy

Prof. S. Butail

Department of Mechanical Engineering, Northern Illinois University, DeKalb IL 60115, U.S.

Prof. E. Caroppo

Department of Mental Health, Local Health Unit ROMA 2, 00159 Rome, Italy

University Research Center He.R.A., Università Cattolica del Sacro Cuore, 00168 Rome, Italy

Prof. Z.-P. Jiang

Department of Electrical and Computer Engineering, Tandon School of Engineering, New York University, 370 Jay Street, Brooklyn NY 11201, U.S.

Prof. A. Rizzo

Department of Electronics and Telecommunications, Politecnico di Torino, 10129 Turin, Italy

Institute for Invention, Innovation and Entrepreneurship, Tandon School of Engineering,
New York University, Six MetroTech Center, Brooklyn NY 11201, U.S.

Prof. M. Porfiri

Center for Urban Science and Progress, Tandon School of Engineering, New York University, 370 Jay Street, Brooklyn, NY 11201, U.S.

Department of Mechanical and Aerospace Engineering , Tandon School of Engineering,
New York University, Six MetroTech Center, Brooklyn NY 11201, U.S.

Department of Biomedical Engineering, Tandon School of Engineering, New York University, Six MetroTech Center, Brooklyn NY 11201, U.S.

Email Address: `mporfiri@nyu.edu`

Our efforts as a society to combat the ongoing COVID-19 pandemic are continuously challenged by the emergence on new virus variants. Variants could be more infectious than existing strains and many of them are also more resistant to available vaccines. The appearance of these new variants cause new surges of infections, exacerbated by infrastructural difficulties, such as shortages of medical personnel or test kits. In this work, we establish a high-resolution computational framework for modeling the simultaneous spread of two COVID-19 variants: a dominant, base variant and a new variant. Our computational framework consists of a detailed database of a representative U.S. town and a high-resolution agent-based model that uses the Omicron variant as the base variant and offers flexibility in the incorporation of new variants. Our results suggest that the spread of new variant can be contained with highly efficacious tests and mild loss of vaccine protection. However, aggressiveness of the ongoing Omicron variant and waning vaccine immunity point to an endemic phase of COVID-19, in which multiple variants will coexist and residents continue to suffer from infections.

1   Introduction

The World has been experiencing reoccurring surges of COVID-19 since the World Health Organization (WHO) proclaimed it a pandemic on March 11th, 2020. [1] Most recently, major waves of infections and deaths have been caused by new mutations of the virus, including the Delta [2] and Omicron [3,4] variants. These emerging variants were more infectious, had shorter latency periods, and were more resistant to existing vaccines than the wild-type variant. [5] Not unexpectedly, each new variant and the resulting wave of infections questioned the preparedness of our healthcare systems and detection infrastructures. [6] Often times, these surges in infections prompted governments to reconsider any lifting of existing restrictions and to devise targeted testing approaches. [6,7]

Since the inception of the COVID-19 health crisis, mathematical models have proved to be fundamental in predicting the course of the pandemic in response to various interventions. [8–12] In particular, they have improved our understanding of COVID-19 spread, [9,13–18] assisted in the implementation of non-pharmaceutical interventions (NPIs), [11,19–22] informed the design of testing and contact tracing campaigns, [16,23–27] helped plan reasonably safe pathways to return to normalcy, [28–30] and guided vaccine roll-outs. [31–35] Recently, models have been used to predict long-term, reoccurring vaccine campaigns and simulate post-pandemic realities — scenarios in which the virus is always present and the disease is endemic. [36–38] Within the study of post-pandemic scenarios, it is paramount to establish models of multiple variants of COVID-19 that could coexist in an endemic setting, as our societies pursue proactive testing and vaccination strategies to mitigate the effects of the virus. [39] The need to study multiple coexisting variants has been documented for several years in the context of influenza. [40] Recent work by Lazebnik and Bunimovich-Mendrazitsky reinforces that such a need is even stronger for understanding the future course of the COVID-19 pandemic. [41] To date, existing research on multi-variant COVID-19 modeling have mostly focused on compartmental models, tailored to predict the interplay between multiple strains and to study the impact of detection effectiveness, NPIs, and vaccines on the ability to contain emerging variants.

A number of efforts have investigated the dominance of different variants based on their infectiousness, [41–46] with theoretical studies grounded in the growing literature of bi- and multi-virus models. [47–49] Predictably, whether it is one or multiple variants that are being

transmitted, testing is key to halt the spread. In particular, Xu et al. [50] investigated different curbing strategies against new variants, stressing out that the effectiveness of good testing and strict quarantine may be comparable with more drastic measures such as stay-at-home orders. On the other hand, there is no consensus regarding the effectiveness of NPIs and vaccines in the presence of multiple strains. With respect to NPIs, some authors have offered evidence in favor of their critical role in multi-variant models. For example, results by Yagan et al. [51] support the key role of masks in curbing the spread, and Arruda et al. [52] observed that a relaxation of restrictions correlates with rapid infection increases. Other authors, instead, reported a weaker role of NPIs on the multi-strain epidemic transmission. For example, Azzizi et al. [53] showed that self-distancing plays a marginal role in mitigating emerging variants that lead to asymptomatic infections. Likewise, Nielsen et al. [54] reported that lockdowns may favor the transmission of less infectious variants. The effectiveness of vaccines has also gathered contrasting results in existing multi-variant models. For example, a study by Bugalia et al. [55] suggested that it is more important that the vaccine is efficacious against the dominant variant, rather than against an emerging one. Contrasting evidence has been offered by De Leon et al. [56], whose model-based approach attributes the spread of the Delta variant to its higher resistance to vaccinations than the dominant Alpha variant. More generally, the critical role of vaccines has been investigated by many studies including: the work of Layton and Sadria [57] on multi-variant COVID-19 spread in Ontario, Canada, the effort by Dutta [58] on the role of vaccines and NPIs on curbing infection surges caused by new variants, and the endeavor by Getz et al. [59] on the waning of vaccine benefits against new variants. Interestingly, Gonzalez and Arenas [60] were successful in timely demonstrating that the Omicron variant could result in large number of infections. The authors attributed the surge to high infectiousness of the variant, suggesting that the vaccine benefits had little impact on the spread.

Compartmental models describe the pandemic via global variables that represents the overall number of individuals in each specific health state and evolve in time according to coupled differential equations describing the progress of the disease. Despite being powerful and mathematically tractable, these models have some inherent limitations due to their coarse-grain resolution. These limitations hinder their applicability to reproduce and study the spread of epidemic diseases in small- or medium-size populations, with their hetero-

geneity in the network of contacts and in the behavior, demographics, and mobility patterns of the residents. In this work, we seek to fill this gap of knowledge by establishing a high-resolution modeling framework set up at the granularity of a single individual for the study of two coexistent COVID-19 variants . The proposed framework includes a detailed database of a medium-sized U.S. town and an agent-based model (ABM) that simulates the spread of two different variants. Our effort concludes a sequence of studies which we initiated at the beginning of the pandemic to empower policy makers with scientifically backed predictions on the effectiveness of testing strategies, NPIs, and vaccines. To date, this approach has been used to elucidate the effectiveness of different vaccination strategies [24], analyze and improve the safety of local reopening efforts [30], investigate the urban design factors that play a role in the spread of an epidemic [18], and study the necessity for booster campaigns. [35]

The present effort shall conclude our line of research by contributing new insight into the future of the pandemic, potentially in the form of an endemic phase in which multiple variants will coexist. Specifically, herein we advance our ABM approach to reproduce the simultaneous spread of two variants of COVID-19 —one being initially dominant, and another one that is emerging— in a partially vaccinated population. We specifically attempt at modeling real-world vaccine uptake, in the form of two-dose vaccines and booster shots, along with their waning immunity. The model is highly flexible and includes many tunable parameters. The two variants can have different levels of infectiousness and the vaccine may not provide equal benefits against them. Specifically, the vaccine protection against infection, virus transmission, development of symptoms and severe, or lethal case of COVID-19 are parameters that can be set differently from one variant to the other. Moreover, we allow for differential capability to detect infected individuals between the two variants. These features allow us to study the effects of main characteristics of a new COVID-19 variant: its infectiousness, resistance against existing vaccines, and ability to evade detection. As such, our framework affords high resolution analysis about the emergence of new COVID-19 strains in a real medium-sized U.S. town with 79,205 inhabitants —New Rochelle, New York— for which we closely replicate residents' lifestyles.

We set our simulations to begin in mid-April 2022 and select Omicron as the initially dominant COVID-19 variant — further referred to as the *base variant* — spread over a popu-

lation whose immunity to COVID-19 is already reduced. We simulate the spread of second variant — further referred to as the *new variant* — under different infectiousness assumptions. Provided that the new variant is less infectious than Omicron, our framework indicates that even with considerable losses in vaccine protection and testing efficacy, our existing healthcare system and infrastructure should be sufficient to resist the spread of the new variant. On the other hand, combating new variants would be harder, if not impossible, in case their infectiousness would exceed the one of Omicron. None of these scenarios points to a disease-free phase: let it be a new variant or the Omicron variant, it is tenable that we will have to endure with COVID-19 in the long run.

2 Methods

Building on our previous efforts, [24, 30, 35] we develop a computational framework that includes two components: a database of the town of New Rochelle and a high-resolution ABM that reproduces the spread of multiple variants of COVID-19. The high-granularity of our computational framework allows us to capture the evolution of the pandemic across locations in the town through contacts and mobility of the town's residents.

The database consists of geographic coordinates of all the residential and public locations in New Rochelle. Locations are divided into six categories: households, workplaces, school buildings, retirement homes, and hospitals, and time-off places. The last category includes locations that residents may visit during off hours for entertainment, leisure, and buying grocery items. The majority of business locations and activities are identified using SafeGraph, [61] following the procedure detailed in. [35] In addition to the locations within the town's administrative limits, the database includes some out-of-town venues frequented by the residents of New Rochelle: workplaces, time-off places, a school, and a retirement home. Finally, the database incorporates information on the public transit routes.

A synthetic population of the town is created using the data available through the United States Census Bureau. [62] The model statistically mirrors the age distribution, household and family structure, and social roles of the actual residents. In total, the synthetic population comprises 79,205 agents, with a one-to-one correspondence with the actual population of New Rochelle. To mimic the real residents of the town, agents are assigned to their

living place, which can be a household, a retirement home, or, for inpatients, a hospital. Agents can go to school or work, depending on their age, and are thus assigned to workplaces and school or college classes. Moreover, agents can visit time-off places, such as grocery stores or movie theaters. Some agents work in neighboring towns and cities, and they commute to work using carpools, public transit, or cycling. The statistical distribution of workplaces and means used to commute is obtained from the U.S. Census Bureau. [62] In addition to time-off places, agents can visit each other in their households. The details on the database and creation of the synthetic population can be found in our earlier works. [24,30,35] The ABM models the spread of two variants (the base and the new variant) of COVID-19 upon contacts between susceptible and infectious agents, which can occur at any of the locations included in the database, as well as during transit. Our simulations start with the base variant spread throughout the population and a single individual infected with the new variant. Agents can become infected with either of the variants. Upon infection, agents may be detected through testing, and subsequently treated via home isolation, routine hospitalization, or hospitalization in an intensive care unit (ICU). The model distinguishes two types of testing: agents can be either tested in their car, or in clinics and hospitals. Testing in clinics or hospitals is assumed to be more risky as the odds of transmitting the virus is evidently higher. The ABM also includes contact tracing, which reflects the CDC guidelines as of April 2022, and according to which fully vaccinated individuals do not need to home isolate upon exposure and possible infection. [63]

The time frame for this study spans three months starting from mid-April 2022, with the base variant being the then dominant Omicron variant. While most of the town was vaccinated, vaccines were less efficacious against the base variant, and their effectiveness was waning for the majority of the residents. [63,64] The economy was fully reopened with no NPIs or other restrictions in place. The effect of second variant was investigated under different assumptions on its infectiousness relative to the base variant. We studied the effects of a reduction in the already waning vaccine protection against the new variant and the declined capability to detect the new variant through testing. The schematic outline of our database and new model features is summarized in Figure 1.
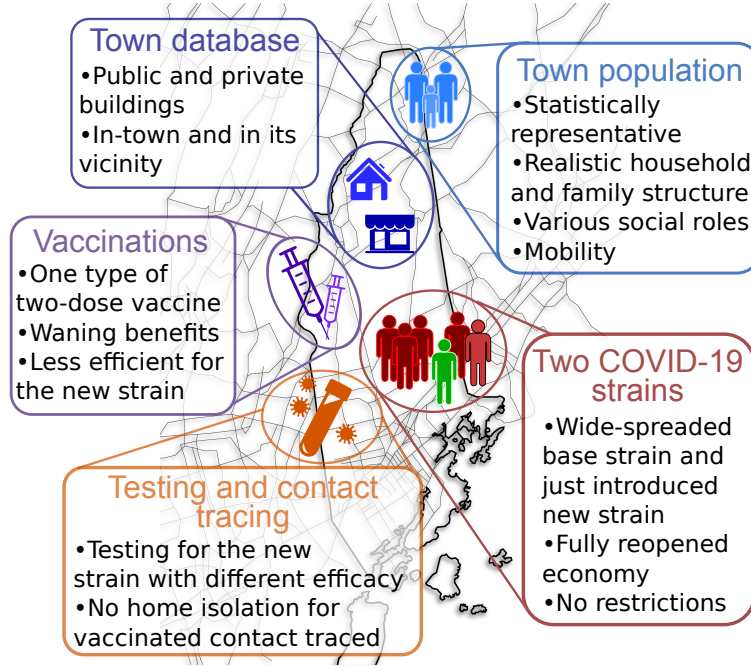
Figure 1: The town of New Rochelle, NY and the highlights of our current computational framework.

2.1 COVID-19 progression model

An agent in our model can be infected with only one variant (variant 1 or 2) of COVID-19 at a time, and, once infected, they may be tested and treated. Recovery from COVID-19 grants the agent a temporary immunity to the variant they were infected with, however, it has no effect on the probability of infection with the other variant.

The detailed progression model is shown in Figure 2. We distinguish several classes of susceptible agents, depending on their previous infection history, vaccination status, and occurrence of COVID-19-like symptoms due to other illnesses, such as influenza. A fraction of agents is susceptible to both variants (S and S^V, where the superscript V denotes vaccinated individuals). Agents who recover from one variant are temporarily susceptible only to the other variant (R_1, R_2, R_1^V, and R_2^V, where the integer subscript denotes the variant). In addition, some susceptible agents experience COVID-19 like symptoms caused by non-COVID-19 diseases; such instances may lead to false positives in testing and detection. Vaccine immunity is modeled through a reduction in the infection capability and a reduced severity of the symptoms. COVID-19-like symptoms may lead to testing and home isolation of an otherwise healthy, susceptible agent.

Once infected, the agents, vaccinated or otherwise, become exposed (E_1, E_2, E_1^V, and E_2^V).

An exposed agent does not show symptoms of the disease, and is less infectious than symptomatic individuals. [65,66] Exposed agents can then either recover as they remain asymptomatic or develop COVID-19 symptoms. Exposed agents can get tested and become home isolated. Testing of all the modeled agents can be done in a car (T_c) or in a hospital (T_{Hs}). Any agent can be contact-traced at any time of the simulation, following the rules described later in this section.

When an agent develops COVID-19 symptoms, they transition to the symptomatic state in their respective variant and vaccination status category (Sy_1, Sy_2, Sy_1^V, and Sy_2^V). Symptomatic agents can be tested and, if they do, they further undergo one of the three treatments distinguished in our model: home isolation (I_{Hm}), normal hospitalization (H_N), and hospitalization in an intensive care unit, ICU (H_{ICU}). The treatment of an agent can change over time, as indicated in the schematic in Fig. 2.

Exposure to the disease may end in a fatal outcome (D) or a full recovery. Once recovered from a variant, the agent becomes temporarily immune to that specific variant. If an agent who is already immune to the base variant becomes infected with the new variant, for some time they are immune to both variants (R and R^V). [63] In the absence of immunity, a recovered agent becomes temporarily immune to the variant they were infected with while remaining susceptible to the other circulating variant (R_1, R_2, R_1^V, R_2^V). Immunity is eventually lost after a fixed amount of time, and the agent becomes susceptible again to both virus variants (S and S^V). In our simulations, the duration of natural immunity is set to 90 days, consistently with the CDC guidelines at the moment of writing this paper. [63] Due to the uncertainty on the estimation of such a duration, however, we performed additional simulations (reported in the Supporting Information) setting it to the most optimistic estimate of 240 days. [67]

The probability that a susceptible agent becomes infected with one of the two variants is a function of the number of agents infected with that variant in all the locations this agent frequents, and on their characteristics. [24,30,35] Specifically, a susceptible agent i can get infected with variant $k = \{B, N\}$ (base and new, respectively) at a time step t with probability

$$p_i^k(t) := 1 - e^{-\Delta t \Lambda_i^k(t)}, \tag{1}$$

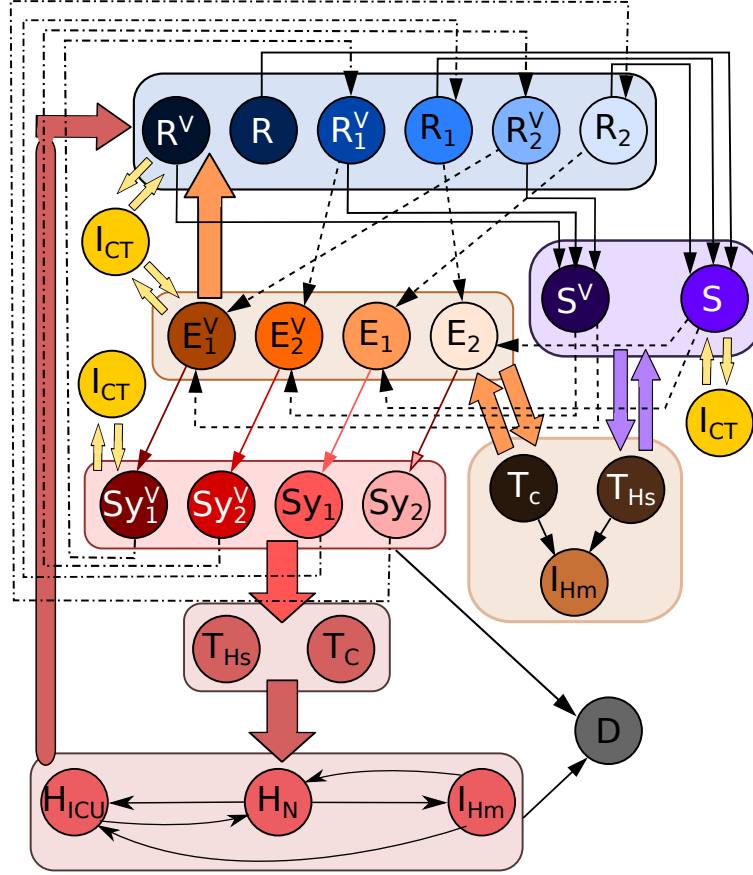where Δt is the duration of one simulation time-step and $\Lambda_i^k(t)$ is a function that repre-

Figure 2: COVID-19 progression with two variants. Subscripts 1 and 2 denote the two different variants; absence of a subscript indicates resistance (R^V and R) or susceptibility to both variants (S^V and S). Superscript V corresponds to vaccinated agents. Thin lines are visually differentiated without specific meaning, to enhance readability. Thick colored lines mark transitions that hold for the entire group. Regardless of their variant type or vaccination statuses, an agent in the model can be susceptible (S), exposed (E), and symptomatic (Sy). Agents can be tested and home isolated (I_{Hm}) with testing being performed in a car (T_c) or in a hospital (T_{Hs}). All the agents can be subject to contact tracing (I_{CT}), resulting in home isolation of unvaccinated individuals and vigilance of others. Exposed agent may recover without ever developing symptoms (R) or become symptomatic after a latency period (Sy). Symptomatic agents can be tested and treated through home isolation (I_{Hm}), normal hospitalization (H_N), or hospitalization in an intensive care unit, ICU (H_{ICU}). The disease ends in either recovery (R) or death (D). Recovery grants temporary immunity against the variant with which the agent was infected.

sents the cumulative level of risk of infection of variant k at time t at the locations where agent i may be present. In our model, we assume that an individual cannot be simultaneously infected with both variants, so that if an individual contracts the base variant at time t (according to (1)), then they cannot contract the new variant at the same time. The general expression for the cumulative risk of infection $\Lambda_i^k(t)$ for agent i reads

$$
\begin{aligned}
\Lambda_i^k(t) := & \lambda_{\text{Hh},f_{\text{Hh}}(i)}^k(t) + \lambda_{\text{W},f_{\text{W}}(i)}^k(t) + \lambda_{\text{Sc},f_{\text{Sc}}(i)}^k(t) + \lambda_{\text{Rh},f_{\text{Rh}}(i)}^k(t) \\
& + \lambda_{\text{Hsp},f_{\text{Hsp}}(i)}^k(t) + \lambda_{\text{Tr},f_{\text{Tr}}(i)}^k(t) + \lambda_{\text{To},f_{\text{To}}(i,t)}^k(t),
\end{aligned}
\tag{2}
$$

where the function $\lambda_{\bullet,\ell}^k(t)$ denotes the contribution to the risk of infection of variant k from location ℓ at time t. The first subscript indicates the type of location, that is, households (Hh), workplaces (W), school buildings (Sc), retirement homes (Rh), hospitals (Hsp), public transit (Tr), and time-off locations (To); the function in the second subscript, $f_\bullet(i)$, maps agent i to the location of type $\bullet$ associated with agent i. Note that some of the agents may not be associated with any location of a specific type $\bullet$. In this case, we assume that $f_\bullet(i) = \emptyset$ and the corresponding contribution to the risk of infection is null, that is, $\lambda_{\bullet,\emptyset}^k(t) = 0$. For instance, if i is a student, then i is not associated with any workplace and $\lambda_{\text{W},f_{\text{W}}(i)}^k(t) = 0$. Finally, we note that the time-off location associated with an agent i is time-varying. More details can be found in our previous work. [24, 30, 35]

The contribution of an in-town location ℓ of type $\bullet$ to the risk of infection of variant k at time t, $\lambda_{\bullet,\ell}^k(t)$, is defined as

$$
\lambda_{\bullet,\ell}^k(t) := \frac{1}{n_\ell^{\alpha_q}} \sum_{j:f_\bullet(j)=\ell} \left(E_{jk}(t)\rho_j\beta_{\bullet,j}^k + Sy_{jk}(t)\psi_\ell c_j\rho_j\beta_{\bullet,j}^k \right),
\tag{3}
$$

where E_{jk} and Sy_{jk} are indicator functions that depend on the infection status of agent j and take values 0 or 1. Specifically, if agent j is infected with variant k and in the exposed state, it holds $E_{jk} = 1$ and $Sy_{jk} = 0$, while if they are showing disease symptoms, it holds $E_{jk} = 0$ and $Sy_{jk} = 1$. Variable $\rho_j \geq 0$ captures the variability in the risk of infection among the agents, $c_j > 1$ quantifies increased risk of infection of an agent with symptoms, n_ℓ is the number of agents, both healthy and infected, at location ℓ, and $\beta_{\bullet,j}^k$ is the transmission rate associated with agent j infected with variant k in a location of type $\bullet$. The contributions of workplaces and time-off locations that are outside of New Rochelle to the risk of infection of variant k are accounted for using estimates on the COVID-19 prevalence in the region. This is a consequence of the fact that our ABM simulates only

the town and does not explicitly model the surrounding area. Agents who frequent neighboring towns have their $\lambda^k_{W,\ell}(t)$ and $\lambda^k_{To,\ell}(t)$ computed based on approximate prevalence of variant k in the region,

$$\lambda^k_{\bullet,\ell}(t) = \beta^k_\bullet \xi^k(t) \chi, \tag{4}$$

where the function $\lambda^k_{\bullet,\ell}(t)$ can be related to either a workplace (W) or a time-off location (To). Parameter χ represents the fraction of the population infected with any COVID-19 variant in the region neighboring the town. Such a fraction is estimated based on the official data on COVID-19 prevalence [68–70] at the beginning of the simulation. To reflect the presence and dynamic changes in the prevalence of each variant, Eq. (4) includes the time-varying quantity $\xi^k(t)$, which is the actual fraction of agents infected with variant k in New Rochelle,

$$\xi^k(t) = \frac{N^k_I(t)}{N^{tot}_I(t)}, \tag{5}$$

where $N^k_I(t)$ is the number of agents infected with variant k at time t and $N^{tot}_I(t)$ is the total number of infected agents at that time - including infections with both the base and the new variant.

The transmission rates for the base variant, which is the Omicron variant (as it accounts for 99.7% of the COVID-19 cases as of mid-April 2022 [71]), in Eqs. (3) and (4) are computed by scaling the transmission rates that we have previously estimated for the Delta variant. [30, 35] In particular, according to infectiousness report by Liu et al., [72] the Omicron variant is characterized by a 2.5 times higher transmissibility than Delta, which we use as the scaling factor for all the transmission rates $\beta^B_{\bullet,i}$. In our study, we test different hypotheses on the risk of infection of the new variant relative to the ease of transmission of the base variant. All the relevant transmission-related parameters are listed in the Supplementary Material.

2.2 Vaccinations

In this study, we consider an advanced phase of the pandemic, in which vaccines have been already developed and made available to a wide portion of the population. For this reason, we assume that individuals have already made their choices on whether to take the vaccine shot or not and, those who decided to vaccinate, were already vaccinated at the moment of starting the simulations. Moreover, we omit possible ongoing vaccination or

booster campaigns that are implemented during the short-term simulation time-horizon. For a study that focuses on this issue, we refer to our previous work. [35] The number of vaccinated agents is determined from the reported data at the county level. [73] We assume that each vaccinated agent received the vaccine some time between January 1st 2021 and the start of the simulations, matching the actual time distribution of the vaccination campaign, [74], as detailed in the Supplementary Material. We also consider that part of the population received a booster shot. Similar to standard vaccines, the number of agents who received the booster is determined from the reported data at the county level, [73] and the time distribution of booster administrations matches the actual time distribution of the booster shot campaign. [74]

Similar to our recent study on waning immunity, [35] vaccines do not grant full immunity and their protection wanes with time. The exact modeling strategy of vaccine benefits for the base variant is the same as described therein. However, the level of protection is reduced following the data reported for Omicron. [75, 76]

Given the uncertainty surrounding the effectiveness of booster shots in preventing infection with Omicron and potential future variants, [76, 77] we present two extreme outcomes: a worst-case scenario with *ineffective booster shots*, for which the booster shot does not provide any additional immunity on top of the benefits already gained with a standard two-shot vaccine; and a best-case scenario with *highly effective booster shots*, for which booster shots restore maximal benefits and their resulting protection does not wane for the time-horizon of our simulations. All details are reported in the Supplementary Material.

In our analysis, vaccines do not necessarily grant the same protection towards the new variant compared to the base variant. We vary the benefits of immunization against the new variant using a single parameter termed *protection loss*, with values between $[0, 1]$. A protection loss of 0 means that the vaccine is as effective against the new variant as against the base variant, while 1 indicates no protection against the new variant.

The protection loss affects all the vaccine benefits. The vaccine grants a reduction in the probability of infection, increased chances of never developing symptoms, reduced transmission rates if infected, and smaller risk of developing a severe or fatal case of COVID-19. Protection loss reduces all these benefits, making the agent more vulnerable to infection and if infected, more infectious and prone to having symptoms, severe or lethal. The exact

expressions for benefits and the effects of protection loss are detailed in the Supplementary Material.

There are no new vaccination doses nor booster shots distributed to the agents during the simulation time frame. Furthermore, contrary to our previous study, [35] fully vaccinated agents are as socially active as the unvaccinated population. This is motivated by the full restoration of local economy and general pre-pandemic levels of mobility and human activity. Finally, vaccinated agents do not need to home isolate when contact-traced, which reflects the CDC guidelines issued during the simulation window. [63]

2.3 Testing and contact tracing

At any point of the infection, an agent can be tested for COVID-19 with a probability that depends on whether the agent is showing symptoms of the disease. An agent showing symptoms due to other illnesses can also undergo testing. Agents are home isolated from the moment they start waiting for the test to the time they get their test results. If the results are positive, their isolation continues and if required, they may get further treatment in a hospital.

Infected agents who are not symptomatic can receive a false negative test result. In this case, they leave their home isolation and continue their normal activities as if they were healthy. The percentage of false negative tests changes across COVID-19 variants. For our current study we consider it to be 0.385%. This represents an average between false negative tests from two most common test types in the region, following estimates for the Omicron variant. [78] To model the impact of the new variant on the detection capabilities of infected individuals we introduce a parameter termed *testing efficacy loss,* equal to the probability of an infected agent to receive a false negative test result. By doing so, we account for the possibility that test kits may have a reduced capability to detect the new variant. Our model also incorporates a form of contact tracing that follows the local guidelines. [63] When an agent receives a positive COVID-19 test result, the agents with whom they were in recent social or professional contexts are contact-traced according to the rules outlined in our previous publication. [35] The difference in the current model is that vaccinated and contact-traced agents are no longer required to quarantine. Instead, they continue their regular lifestyles while staying vigilant for a recommended duration of 15 days. This im-

plies that if these agents develop COVID-19 symptoms, they will immediately isolate and sign up for a test. On the other hand, agents that are not vaccinated quarantine for five days and remain vigilant for another 10 days.

2.4 Simulation setup

To approximate the epidemic situation in the town as of April 2022, we initialize the simulations with three types of agents infected with the base variant: i) agents who are exposed, but undetected, and may develop disease symptoms; ii) agents who are asymptomatic and possibly detected and quarantined; and iii) agents who have symptoms and are being in various stages of testing and treatment. In addition, part of the agents are considered to have recently recovered from COVID-19 and carry a temporary natural immunity against the base variant. Recovery occurs at a randomly selected day within a three month window. [63]

We estimate the number of agents in each of four categories using the data on infected agents reported for the region. [74] The exact source and numbers of initially infected agents are listed in the Supplementary Material. Simulations start with a single seed agent infected with the new variant and no COVID-19 symptoms — if this agent ends up developing symptoms, they can be detected through testing.

After some initial simulations, which span a one-year period from mid-April 2022, we restrict our simulation-window to a three-month time-horizon, for which we perform extensive Monte Carlo simulations. As of mid-April 2022, most of the residents who wanted to receive a vaccine and (possibly) a booster shot were already vaccinated against the base variant. However, vaccine benefits of many of the residents were already waning. Social activity was restored to pre-pandemic levels and no NPIs were in place. At the beginning of the simulations, some agents have a natural immunity against the base variant, due to previous recovery, and a number of agents were infected with the base variant, in any stage of the disease. The number of these agents is estimated from, [74] with a procedure similar to the one detailed in our previous work. [24, 30, 35]

To measure the impact of the new variant, we count the total number of infections in the town after the three month period under different scenarios of protection loss and test efficacy loss. Furthermore, we examin three different scenarios, in which the new variant is i)

twice less infectious, ii) *equally infectious*, or iii) *twice more infectious* than the base vari-
ant. These scenarios are obtained by changing the transmission rates for the new variant,
as detailed in the Supplementary Material.

3   Results

Here, we illustrate our main simulation results. First, we study the long-term evolution
of the disease by simulating the ABM over a period of one year. These simulations sug-
gest that an endemic phase is extremely hard to be avoided. Afterwards, we focus on pre-
dicting the total number of infections over the three-month simulation period and show
that, under most realistic scenarios, on average almost every town resident becomes in-
fected at least once during the three-month period. Finally, we investigate the spread of
the two variants separately to shed light on how the characteristics of the new variant are
conducive to its spread. Our findings suggest that, in many cases, even less infectious vari-
ants could cause massive outbreak, but improved detection and vaccine efficacy may be ef-
fective in curbing the spread of the new variant.

3.1   Simulations predict the emergence of endemic COVID-19

In order to study the long-term evolution of multiple COVID-19 strains, we simulate its
spread for a one-year time-span in two distinct scenarios: one in which booster shots are
ineffective and the new variant is quite infectious, and one in which we assume highly ef-
fective booster shots and a mild new variant. The output of two representative simulations
obtained in these scenarios are illustrated in Figure 3.
For both scenarios, Figs. 3a) and d) show that the disease becomes endemic, since the epi-
demic prevalence never settles to a disease-free state. Moreover, the simulations suggest
that recurrent outbreaks may occur, yielding multiple epidemic waves. Interestingly, the
results of our simulations depict that a competition between the two variants may occur,
whereby, in the long run, only one of them becomes dominant, while the other is eradi-
cated.
Predictably, the variant that will dominate is determined by the effectiveness of booster
shots and on the infectiousness on the new variant with respect to the base one. In partic-
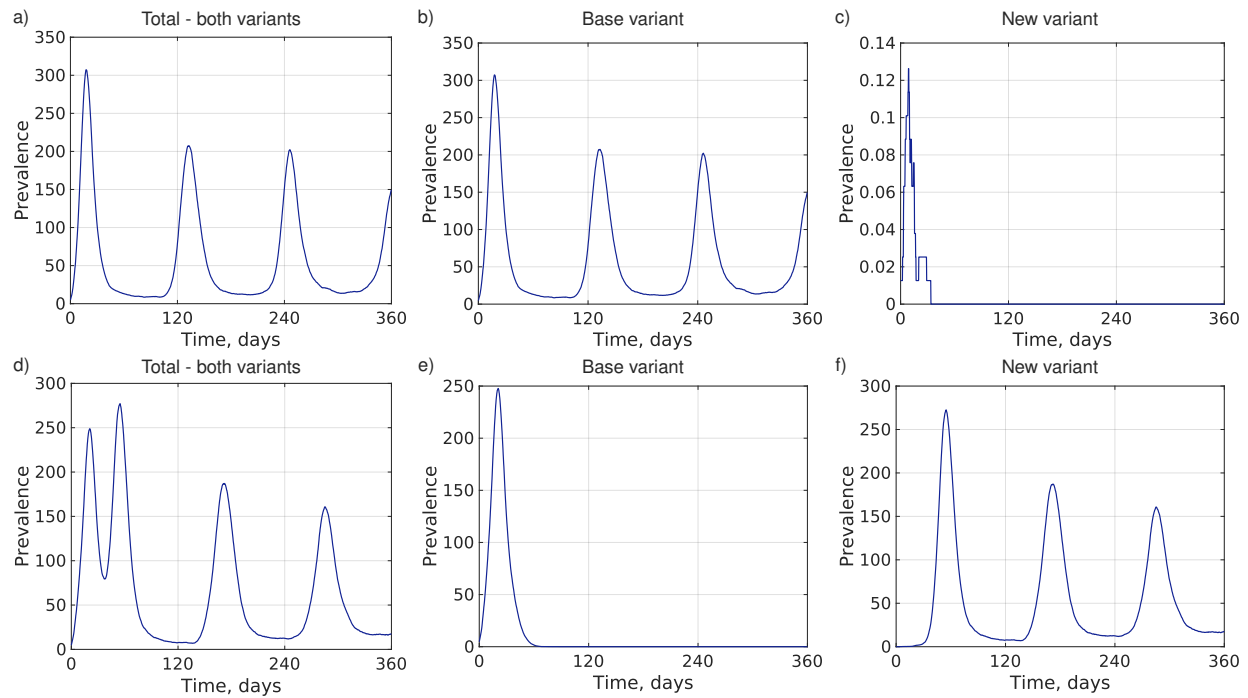
Figure 3: Prevalence of COVID-19 infections after a year-long simulation period for two different scenarios: a-c) ineffective booster shots and new variant less infectious than the base variant; and d-f) perfect booster shots with both variants equally infectious. In both scenarios, we assume 50% protection loss and 50% testing efficacy loss. The plots show the number of infections with both base and new variants per 1000 agents for one realization.

ular, in the case of ineffective booster shots and mild new variants, the base variant will re-
main endemic in the town population (see Fig. 3b)), while the new variant is quickly eradi-
cated (see Fig. 3c)). On the contrary, if booster shots are highly effective and the new vari-
ant is sufficiently infectious, the opposite behavior is recorded (see Figs. 3e) and f)): after
a brief period, the base variant is eradicated, but the new one will remain endemic in the
population.

3.2   Massive numbers of new COVID-19 infections are unavoidable in the pres-
ence of multiple strains

Our preliminary simulations, reported in Fig. 3, suggested that it is extremely difficult to
avoid a long-term endemic phase for the disease. However, they also show that the char-
acteristics of the new variant and of the booster shots may strongly impact the evolution
of the epidemic. For this reason, we further explore this issue by inspecting a wide range
of scenarios. Specifically, we consider different infectiousness of the new variant and effec-
tiveness of booster shots, and we vary the protection loss and the testing efficacy loss in
their entire range of admissible values. In these simulations, we focus on a shorter time pe-
riod of three months starting from mid-April 2022, over which it is reasonable to assume
that neither new variants appear nor updated booster shots campaigns are implemented.
This enables us to derive quantitative estimations on the number of new infections under
different scenarios and compare them. Moreover, such a shorter simulation period allows
us to achieve a sufficiently large number of independent simulations to average the natural
stochasticity of the ABM via Monte Carlo methods.

The total number of COVID-19 infections across both variants is shown in Fig. 4. In all
cases, the total infection count is extremely high. In fact, on average, almost each town
resident becomes infected with one of the two variants at least once during the simulation
and, in some scenarios, even more than once. First of all, by comparing Figs. 4a)–c) with
Fig. 4d)–f), we observe that the efficacy of the booster shot plays a secondary role on the
total number of COVID-19 infections across both variants. Even comparing two extreme
scenarios —a worst-case scenario where booster shots provide no benefit and a best-case
scenario where booster shots restore maximal, non-waning immunity— we register not more
than a 15% decrease in the total number of infections. Moreover, the effects of losses in

protection and testing efficacy are qualitatively unchanged between these two outcomes for the booster shots.

When the new variant is less infectious than the base one (see Fig. 4a) and Fig. 4d)), moderate protection and detection losses visibly reduce the case count. In particular, if the protection loss is not larger than 50%, a considerable drop in the case count can be achieved, even in the presence of a large amount of false negative tests, of the order of 40-50%. In the scenarios where the new variant is equally or more infectious than the base one, our simulations suggest that the disease always becomes endemic, infecting almost the entire population. Moreover, many residents become infected with both variants or re-infected with the same one, as indicated by the fact that the total case count could even exceed the town's population, reaching more than 1000 cases per thousand individuals.

3.3   Improved detection and vaccine efficacy can curb the spread of the new variant

In Fig. 3, we observ that, while an endemic phase for the disease can hardly be avoided, the competition between the two variants may be leveraged to avoid the spread of new, potentially more lethal, variants. In the following, we further investigate this possibility by exploring how detection rate and vaccine efficacy can sensibly reduce the infection count for new variants.

Figure 5 displays the total number of infections due to each of the two circulating variants. The contrasting heat-maps show that the variants interact with each other, whereby an increase in agents exposed to one variant causes a drop of infections with the other. By comparing the top and bottom panels, we observe that the efficacy of booster shots has a marginal, yet tangible, impact on the total number of infections for the base variant — for which a highly effective booster could reduce the infection by no more than 20% — and almost no impact on the total number of cases for the new variant. The overall spreading of the epidemic remains unchanged across the different scenarios — even in the most favorable case, a disease-free phase is not observed.

The total number of infections due to the base variant reaches over 540 cases per thousand individuals in all the considered scenarios, while the contribution from the new variant grows with its infectiousness. If the new variant presents reduced infectiousness, then a
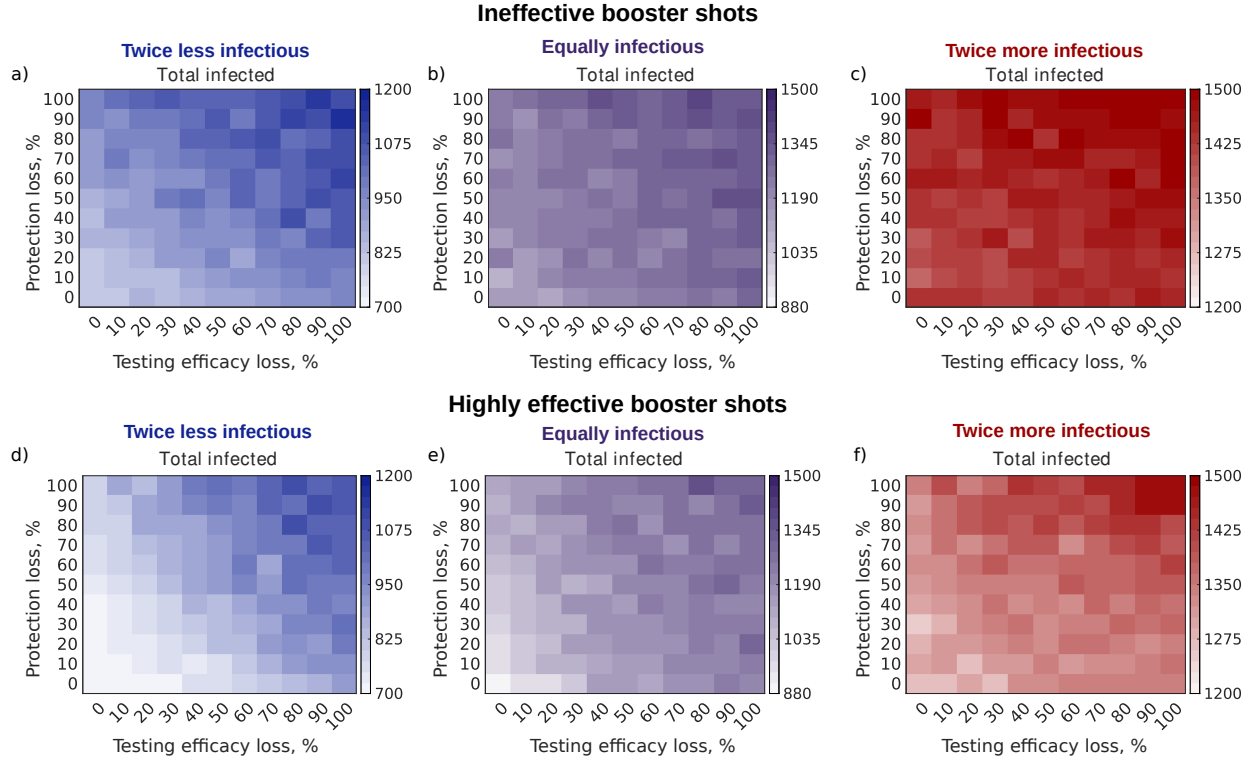
Figure 4: COVID-19 infections during the three-month simulation period as a function of protection and testing efficacy losses. The heat-maps show the number of infections with both base and new variants per 1000 agents after three months of simulations, averaged over 100 realizations. The top and bottom panels display different outcomes of booster shots: ineffective in a)–c), and highly effective in d)–f). The left, central, and right panels pertain to different infectiousness of the new variant relative to the base variant, which is less infectious in a) and d), equally infectious in b) and e), and more infectious in c) and f). A version of this figure with a common color-scale for all the panels is reported in the Supplementary Information (Fig. S4).

high efficacy of tests and vaccines protection would lead to a considerable drop in the number of infections. In fact, if the testing efficacy loss is lower than 50% and the loss of vaccine protection is moderate (that is, less than 30%), then the cumulative number of cases of the new variant remains bounded, even in the absence of any interventions. Therefore, severe propagation of the new variant could be avoided even against protection and testing efficacy at moderate levels, provided that the new variant is less infectious than the base one. However, the total infection count could still be large due to the spread of the base variant. The case count rises with infectiousness of the new variant, with little effect of improved testing detection or protection from vaccines.

In all the simulations included in this section, the natural immunity of the residents is set to 90 days, representing the conservative estimate provided by the CDC guidelines. [79]. Such a choice could be considered as a worst-case scenario, and it could potentially lead to an overestimation of the number of reinfections. To investigate the impact of such a modeling choice on the output of our numerical study, we perform additional simulations in which the duration of natural immunity is extended to an optimistic estimate of 240 days, consistent with the longest estimate in the clinical literature. [80] The results of these additional simulations (reported in Figs. S2 and S3 in the Supplementary Information) are consistent with the findings described herein and show only marginal differences in the total infection count. This suggests that the duration of natural immunity has a secondary impact on the overall emergent behavior of the epidemic process: even under a very optimistic estimate of the duration of natural immunity, an endemic disease can hardly be avoided.

4   Discussion and conclusions

In this work, we establish a novel high-resolution computational framework to study the spread of two COVID-19 variants: a scenario that is recurring globally. The framework is built upon our previous efforts [24,30,35], expanding the ABM developed therein to study the concurrent spread of two types of COVID-19 variants — an initially dominant base variant and an emerging new variant. The framework complements the existing toolbox to study multi-variant spreading, by offering key advantages that are inherent to high-resolution
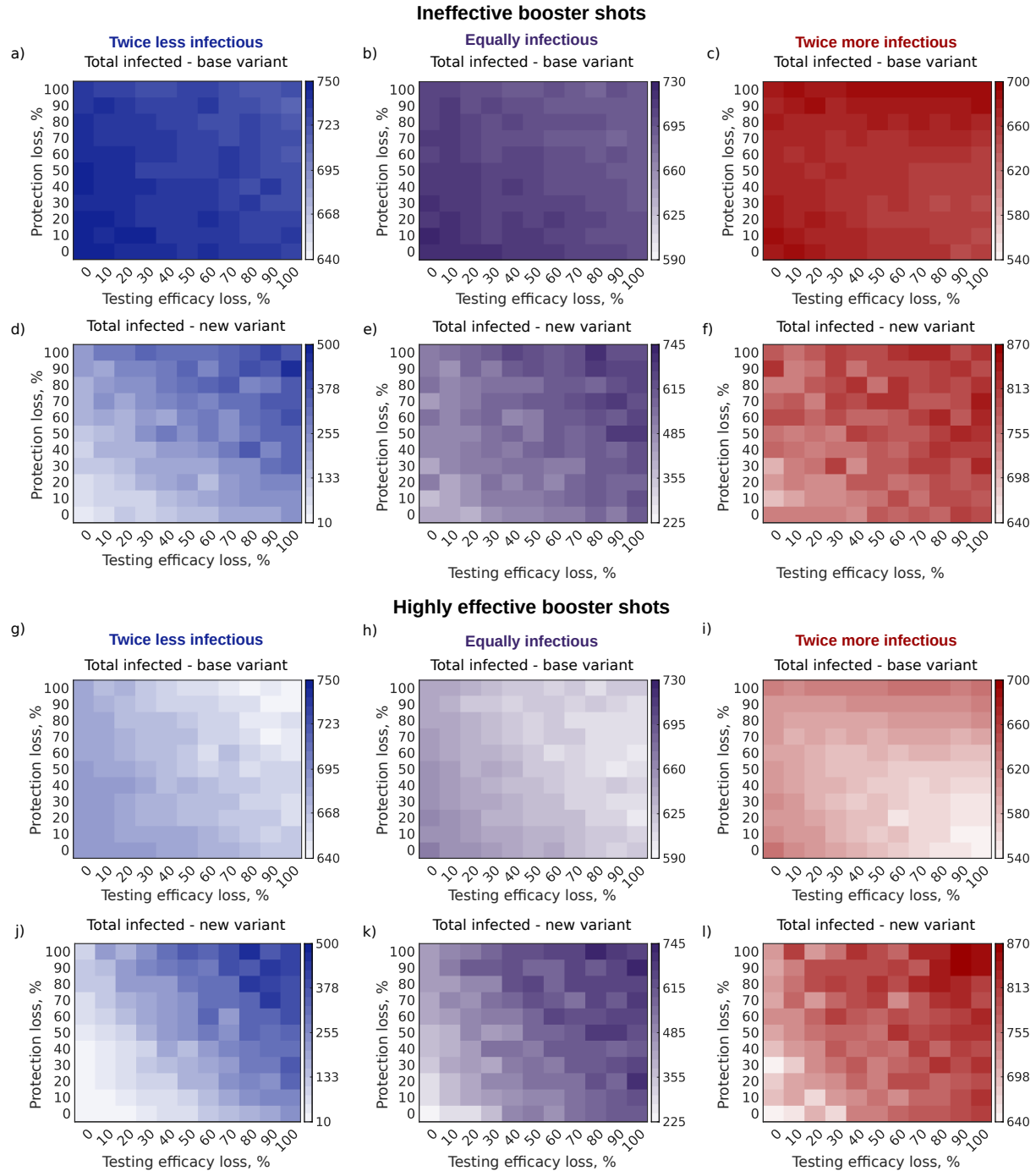
Figure 5: Contributions of each variant to the total number of COVID-19 infections during the three-month simulation period as a function of protection and testing efficacy losses. The heat-maps show the number of infections per 1000 agents with both base and new variants after three months of simulations, averaged over 100 realizations. The set of six top and six bottom panels display different outcomes of booster shots: ineffective in a)–f), and highly effective in g)–l). The left, central, and right panels pertain to different infectiousness of the new variant relative to the base variant which is less infectious in a), d), g), and j); equally infectious in b), e), h), and k); and more infectious in c), f), i), and l). Note that limits of the color-map for the heat-maps are adjusted to the infectiousness of the new variant. A version of this figure with a common color-scale for all the panels is reported in the Supplementary Information (Fig. S5).

ABMs. First, it provides the ability to simulate the spread of infectious diseases given highly heterogeneous, and realistic, human lifestyles and mobility. Second, in resolving individual buildings, professions, and institutions of a real location, our framework opens opportunities for highly granular studies of various aspects of the pandemic such as interventions or vaccinations in towns with similar layouts.

We demonstrate the potential of our modeling approach by applying it to the town of New Rochelle, NY, which was the location of one of the first COVID-19 outbreaks in the U.S. We used the proposed model to study the spread of a hypothetical new variant of COVID-19, concurrently with the Omicron variant, which is the dominant variant as of Spring 2022. The infectiousness and detection characteristics of the new variant were considered as model parameters in a series of what-if studies, exploring vaccine and testing efficacy of the new variant.

In our simulations, the number of infections with the Omicron (base) variant would always reach over half of the population. We attribute such a dramatic level of infection to the reduced effectiveness of vaccines against Omicron, as well as to the documented waning vaccine benefits. While the number of infections with the Omicron variant might have been inflated, intensive spread was not unrealistic. The occurrence of Omicron causes a record spike in the detected cases in the region during winter 2021/2022 and rise of infections is also recorded during the period of the study, amidst waning vaccine benefits, restored normalcy, and the presence of even more infectious subvariants [74].

The introduction of the new variant causes a visible increase in the case count, with the two variants interacting with each other. When the new variant is equally or more infectious than the base variant, even high detection rates and effective vaccines against the new variant fails in reducing the total number of infections. Interestingly, such a dramatic increase is often observed also in the scenario of less infectious variants. This could have been anticipated, given the waning immunity of the vaccine against the base variant and the incomplete adoption of booster shots.

Finally, we identify conditions under which the spread of the new variant could be curbed. Specifically, if the risk of infection of the new variant is lower than the base variant, the combination of sufficiently effective testing and vaccines against the new variant may reduce a new, potential wave. In fact, if protection loss were 40-50% or less, and the false

negativity rate would below 50%, only a tenth of the residents would become infected with the new variant. This number could be further abated, if the vaccine were almost as efficacious against the new variant as it is towards the base variant and the testing and detection infrastructure are highly efficacious.

The results of our numerical simulations are in line with the trends reported in the literature. Significant case rise associated with emergence of new variants were observed by many studies to date, given the fully reopened economy and heavily relaxed quarantining regulations. [52,57,59,60]. Arruda et al. performed numerical simulations within a compartmental model, reporting doubling case counts and occurrences of new infection surges due to the emergence of new variants amidst lifting or absence of restrictions. [52] Using a computational model, Layton and Sandria showed that a new variant that is more infectious and vaccine resistant could infect large portions of the population and strain the healthcare infrastructure. [57] Similarly, through numerical simulations of Omicron as a new variant, Gonzalez and Arenas reported emerging surges of infections for a wide range of hypothetical infectivities and vaccine resistance combinations. [60]

With respect to vaccine efficacy, several studies used compartmental models to support that increasing vaccine efficacy would be a critical factor in curbing the spread of the new variant. [55–58] This is in agreement with our results from the scenario where the new variant is less infectious than the base one. On the other hand, some authors pointed out the inability of vaccines to curb the spread of the new variant under the conditions of waning immunity and with its sufficient infectiousness. [59,60] Prominently, Gonzalez and Arenas showed that if a new variant is equally or or more infectious than the base one, increasing vaccine effectiveness has almost no effect on the final case count. [60] These findings are in line to what we reported for equivalent infectiousness scenarios.

While insightful and consistent with similar efforts, our results should be interpreted while keeping in mind several limitations of the model. First, following CDC recommendations, [63] we set the duration of immunity after recovery to 90 days. This estimate may be conservative, inevitably leading to several re-infections. Although not conclusive for Omicron, there are observations of immunity lasting two or even three times our estimate. [81,82] However, as shown in the additional simulations reported in the Supporting Information, even very optimistic assumptions on the duration of natural immunity would not yield contrasting

conclusions to our study.

The second limitation concerns the limited amount of information about and the high levels of uncertainty on the efficacy of booster shots against variants and the rate at which the immunity wanes after taking the booster shot. [75,76,83] In our study, we partially address this issue by considering two extreme outcomes for the booster shot: a worst-case scenario where booster shots do not provide any benefits, and a best-case scenario where, instead, they restore maximal and permanent immunity. Importantly, we observe that the results of our simulations remain consistent across these two extreme options, with booster shot playing a marginal role on the case count. As of July 2022, novel Omicron-adapted booster shots are being developed by different manufacturers. [84,85] The use of these booster shots, if efficacious, may steer the course of the pandemic. We would like to comment that, even though these booster shots are not currently considered in our model, the flexibility of our computational framework allows for their straightforward implementation, similar to vaccination and booster campaigns incorporated in our previous studies. [35]

Finally, our model does not consider cross-immunity, that is, recovery from an infection with one variant does not yield any natural protection against the other variant. Lack of cross-immunity is not an uncommon assumption in the literature, [41,42,51,52,55,56,58] as it can be viewed as a worst-case, conservative scenario, which is, however, not too distant from what is suspected with the most recent variants. [86–88]

Despite its shortcomings, the high granularity of our model and its faithful representation of the town and its population are key vantage points. Our framework simulates characteristics, lifestyles, and mobility patterns of every individual in the community. It introduces concrete locations, where people interact and the disease spreads, and allows for studying the epidemic in a highly resolved, heterogeneous setting, which is absent from the above mentioned population-based approaches. The framework models contacts between individuals, but, different from network models, it also provides interaction details. The key elements of our framework — realistic vaccinations, variant-dependent testing, and COVID-19 oriented treatment — yield the opportunity for studying the co-evolution of two variants, allocation of resources, and formulation of strategies in times of crisis, such as the most recent Omicron one. [6]

We demonstrate the capabilities of our framework by modeling the interplay of two COVID-

19 variants, along with the effect of waning vaccine immunity and reduced detection on the course of the pandemic. The prediction of aggressive spread of both variants in a practically not immune population, in the absence of NPIs, warrants caution and reconsideration of reinstating at least some protective measures. Distributing further doses of vaccine should also be contemplated, as well as developing new vaccines, more effective against the new variants. Finally, our results indicate that a new wave of infections caused by an emerging variant can be greatly reduced if the variant is less infectious, while the tests and vaccines are only moderately less efficacious. While not unexpected, these conclusions provide a starting point for future studies and "what-if" scenarios that our two variant computational framework can provide, including more extensive studies on the competition between the different variants and the development of model-informed intervention policies to contain the spread of both variants.

Supporting information

Supporting Information is available from the Wiley Online Library or the corresponding author. The complete computational framework, including code needed to reproduce the study is openly available. The database is accessible in Zenodo at `https://doi.org/10.5281/zenodo.5659785`, the agent-based model in Github at `https://github.com/Dynamical-Systems-Laboratory/DSL-ABM-TwoVariants`.

Author contributions

Conceptualization—AT, LZ, SB, AR, MP; data curation—AT, SB; methodology—AT, LZ, SB, AR, MP; software—AT; validation—AT; formal analysis—all the authors; investigation—all the authors; resources—MP; writing—original draft preparation—AT; writing—review and editing—LZ, SB, EC, AR, MP; visualization—AT; supervision—SB, EC, ZPJ, AR, MP; project administration—MP; funding acquisition—SB, ZPJ, AR, MP.

Conflict of interest

The authors declare no conflict of interest.

References

[1] World Health Organization, WHO coronavirus disease (COVID-19) dashboard, available at `https://covid19.who.int`, (Accessed: October 2022).

[2] K. Kupferschmidt, M. Wadman, *Science* **2021**, *372*, 6549, 1375.

[3] D. Tian, Y. Sun, H. Xu, Q. Ye, *J. Med. Virol.* **2022**, *94*, 6, 2376.

[4] F. Rahimi, A. T. B. Abadi, *Int. J. Surg.* **2022**, *99*, 106261.

[5] L. Liu, S. Iketani, Y. Guo, J. F.-W. Chan, M. Wang, L. Liu, Y. Luo, H. Chu, Y. Huang, M. S. Nair, et al., *Nature* **2022**, *602*, 7898, 676.

[6] E. S. Amirian, *J. Public Health Policy* **2022**, 1–5.

[7] P. Yuan, E. Aruffo, Y. Tan, L. Yang, N. H. Ogden, A. Fazil, H. Zhu, *Infect. Dis. Model.* **2022**, *7*, 2, 83.

[8] E. Estrada, *Phys. Rep.* **2020**, *869*, 1.

[9] A. Vespignani, H. Tian, C. Dye, J. O. Lloyd-Smith, R. M. Eggo, M. Shrestha, S. V. Scarpino, B. Gutierrez, M. U. G. Kraemer, J. Wu, K. Leung, G. M. Leung, *Nat. Rev. Phys.* **2020**, *2*, 279.

[10] A. L. Bertozzi, E. Franco, G. Mohler, M. B. Short, D. Sledge, *Proc. Natl. Acad. Sci. USA* **2020**, *117*, 29, 16732.

[11] F. Parino, L. Zino, M. Porfiri, A. Rizzo, *J. R. Soc. Interface* **2021**, *18*, 175, 20200875.

[12] F. Napolitano, X. Xu, X. Gao, *Brief. Bioinform.* **2022**, *23*, 1, bbab456.

[13] I. Bâldea, *Adv. Theory Simul.* **2020**, 2000132.

[14] M. Gilbert, G. Pullano, F. Pinotti, E. Valdano, C. Poletto, P.-Y. Boëlle, E. D'Ortenzio, Y. Yazdanpanah, S. P. Eholie, M. Altmann, B. Gutierrez, M. U. G. Kraemer, V. Colizza, *Lancet* **2020**, *395*, 10227, 871.

[15] G. Giordano, F. Blanchini, R. Bruno, P. Colaneri, A. Di Filippo, A. Di Matteo, M. Colaneri, *Nat. Med.* **2020**, *26*, 6, 855.

[16] F. Pinotti, L. Di Domenico, E. Ortega, M. Mancastroppa, G. Pullano, E. Valdano, P.-Y. Boëlle, C. Poletto, V. Colizza, *PLOS Med.* **2020**, *17*, 7, 1.

[17] A. Arenas, W. Cota, J. Gómez-Gardeñes, S. Gómez, C. Granell, J. T. Matamalas, D. Soriano-Paños, B. Steinegger, *Phys. Rev. X* **2020**, *10*, 041055.

[18] A. Truszkowska, M. Fayed, S. Wei, L. Zino, S. Butail, E. Caroppo, Z.-P. Jiang, A. Rizzo, M. Porfiri, *J. Urban Health* **2022**, 1–13.

[19] N. M. Ferguson, D. Laydon, G. Nedjati-Gilani, N. Imai, K. Ainslie, S. B. Marc Baguelin, A. Boonyasiri, Z. Cucunubá, G. Cuomo-Dannenburg, A. Dighe, I. Dorigatti, H. Fu, K. Gaythorpe, W. Green, A. Hamlet, W. Hinsley, L. C. Okell, S. van Elsland, H. Thompson, R. Verity, E. Volz, H. Wang, Y. Wang, C. W. Patrick GT Walker, P. Winskill, C. Whittaker, C. A. Donnelly, S. Riley, A. C. Ghani, Impact of non-pharmaceutical interventions (NPIs) to reduce COVID-19 mortality and health-care demand, Report of the Imperial College London, UK (`https://doi.org/10.255 61/77482`), **2020**.

[20] F. Della Rossa, D. Salzano, A. Di Meglio, F. De Lellis, M. Coraggio, C. Calabrese, A. Guarino, R. Cardona-Rivera, P. De Lellis, D. Liuzza, F. Lo Iudice, G. Russo, M. di Bernardo, *Nat. Comm.* **2020**, *11*, 1, 5106.

[21] R. Hinch, W. J. M. Probert, A. Nurtay, M. Kendall, C. Wymant, M. Hall, K. Lythgoe, A. Bulas Cruz, L. Zhao, A. Stewart, L. Ferretti, D. Montero, J. Warren, N. Mather, M. Abueg, N. Wu, O. Legat, K. Bentley, T. Mead, K. Van-Vuuren, D. Feldner-Busztin, T. Ristori, A. Finkelstein, D. G. Bonsall, L. Abeler-Dörner, C. Fraser, *PLOS Comput. Biol.* **2021**, *17*, 7, 1.

[22] N. Perra, *Phys. Rep.* **2021**, *913*, 1.

[23] Z. Du, A. Pandey, Y. Bai, M. C. Fitzpatrick, M. Chinazzi, A. Pastore y Piontti, M. Lachmann, A. Vespignani, B. J. Cowling, A. P. Galvani, L. A. Meyers, *Lancet Public Health* **2021**, *6*, 3, e184.

[24] A. Truszkowska, B. Behring, J. Hasanyan, L. Zino, S. Butail, E. Caroppo, Z.-P. Jiang, A. Rizzo, M. Porfiri, *Adv. Theory Simul.* **2021**, *4*, 3, 2170005.

[25] A. Bilinski, F. Mostashari, J. A. Salomon, *JAMA Netw. Open* **2020**, *3*, 8, e2019217.

[26] M. E. Kretzschmar, G. Rozhnova, M. C. J. Bootsma, M. van Boven, J. H. H. M. van de Wijgert, M. J. M. Bonten, *Lancet Public Health* **2020**, *5*, 8, e452.

[27] B. J. Quilty, S. Clifford, J. Hellewell, T. W. Russell, A. J. Kucharski, S. Flasche, W. J. Edmunds, K. E. Atkins, A. M. Foss, N. R. Waterlow, K. Abbas, R. Lowe, C. A. B. Pearson, S. Funk, A. Rosello, G. M. Knight, N. I. Bosse, S. R. Procter, G. R. Gore-Langton, A. Showering, J. D. Munday, K. Sherratt, T. Jombart, E. S. Nightingale, Y. Liu, C. I. Jarvis, G. Medley, O. Brady, H. P. Gibbs, D. Simons, J. Williams, D. C. Tully, S. Flasche, S. R. Meakin, K. Zandvoort, F. Y. Sun, M. Jit, P. Klepac, M. Quaife, R. M. Eggo, F. G. Sandmann, A. Endo, K. Prem, S. Abbott, R. Barnard, Y.-W. D. Chan, M. Auzenbergs, A. Gimma, C. J. Villabona-Arenas, N. G. Davies, *Lancet Public Health* **2021**, *6*, 3, e175.

[28] A. Aleta, D. Martín-Corral, A. Pastore y Piontti, M. Ajelli, M. Litvinova, M. Chinazzi, N. E. Dean, M. E. Halloran, I. M. Longini Jr, S. Merler, A. Pentland, A. Vespignani, E. Moro, Y. Moreno, *Nat. Hum. Behav.* **2020**, *4*, 964.

[29] P. T. Gressman, J. R. Peck, *Math. Biosci.* **2020**, *328*, 108436.

[30] A. Truszkowska, M. Thakore, L. Zino, S. Butail, E. Caroppo, Z.-P. Jiang, A. Rizzo, M. Porfiri, *Adv. Theory Simul.* **2021**, *4*, 9, 2100157.

[31] K. M. Bubar, K. Reinholt, S. M. Kissler, M. Lipsitch, S. Cobey, Y. H. Grad, D. B. Larremore, *Science* **2021**, *371*, 6532, 916.

[32] P. C. Jentsch, M. Anand, C. T. Bauch, *Lancet Infect. Dis.* **2021**, *21*, 8, 1097.

[33] G. Giordano, M. Colaneri, A. Di Filippo, F. Blanchini, P. Bolzern, G. De Nicolao, P. Sacchi, P. Colaneri, R. Bruno, *Nat. Med.* **2021**, *27*, 6, 993.

[34] F. Parino, L. Zino, G. C. Calafiore, A. Rizzo, *Int. J. Robust Nonlinear Control* **2021**.

[35] A. Truszkowska, L. Zino, S. Butail, E. Caroppo, Z.-P. Jiang, A. Rizzo, M. Porfiri, *Adv. Theory Simul.* **2022**, *5*, 6, 2100521.

[36] F. Song, M. O. Bachmann, *BMJ Open* **2021**, *11*, 11, e053507.

[37] F. G. Sandmann, N. G. Davies, A. Vassall, W. J. Edmunds, M. Jit, F. Y. Sun, C. J. Villabona-Arenas, E. S. Nightingale, A. Showering, G. M. Knight, K. Sherratt, Y. Liu, K. Abbas, S. Funk, A. Endo, J. Hellewell, A. Rosello, R. Lowe, M. Quaife, A. Gimma, O. Brady, J. Williams, S. R. Procter, R. M. Eggo, Y.-W. D. Chan, J. D. Munday, R. C. Barnard, G. R. Gore-Langton, N. I. Bosse, N. R. Waterlow, C. Diamond, T. W. Russell, G. Medley, S. Flasche, K. E. Atkins, K. Prem, D. Simons, M. Auzenbergs, D. C. Tully, C. I. Jarvis, K. van Zandvoort, S. Abbott, C. A. B. Pearson, T. Jombart, S. R. Meakin, A. M. Foss, A. J. Kucharski, B. J. Quilty, H. P. Gibbs, S. Clifford, P. Klepac, *Lancet Infect. Dis.* **2021**, *21*, 7, 962.

[38] R. Li, O. N. Bjørnstad, N. C. Stenseth, *R. Soc. Open Sci.* **2021**, *8*, 6, 210292.

[39] O. Akman, S. Chauhan, A. Ghosh, S. Liesman, E. Michael, A. Mubayi, R. Perlin, P. Seshaiyer, J. P. Tripathi, *Bull. Math. Biol.* **2022**, *84*, 1, 1.

[40] A. J. Kucharski, V. Andreasen, J. R. Gog, *J. Math. Biol.* **2016**, *72*, 1, 1.

[41] T. Lazebnik, S. Bunimovich-Mendrazitsky, *PLOS ONE* **2022**, *17*, 4, e0260683.

[42] M. Fudolig, R. Howard, *PLOS ONE* **2020**, *15*, 12, e0243408.

[43] F. Xia, X. Yang, R. A. Cheke, Y. Xiao, *Infect. Dis. Model.* **2021**, *6*, 988.

[44] M. Massard, R. Eftimie, A. Perasso, B. Saussereau, *J. Theor. Biol.* **2022**, *545*, 111117.

[45] S. Cao, P. Feng, W. Wang, Y. Shi, J. Zhang, *Nonlinear Dyn.* **2021**, *106*, 2, 1557.

[46] D. A. Burbano Lombana, L. Zino, S. Butail, E. Caroppo, Z.-P. Jiang, A. Rizzo, M. Porfiri, *Applied Network Science* **2022**, *7*, 1, 66.

[47] J. Liu, P. E. Paré, A. Nedić, C. Y. Tang, C. L. Beck, T. Başar, *IEEE Trans. Autom. Control* **2019**, *64*, 12, 4891.

[48] J. Chen, Y. Huang, R. Zhang, Q. Zhu, *IEEE Trans. Signal Inf. Process. Netw.* **2021**, *7*, 294.

[49] M. Ye, B. D. O. Anderson, J. Liu, *SIAM J. Control Optim.* **2022**, *60*, 2, S323.

[50] L. Xu, H. Zhang, H. Xu, H. Yang, L. Zhang, W. Zhang, F. Gu, X. Lan, *Nonlinear Dyn.* **2021**, *105*, 3, 2757.

[51] O. Yagan, A. Sridhar, R. Eletreby, S. Levin, J. B. Plotkin, H. V. Poor, *Harvard Data Science Review* **2021**, *Special Issue 1.*

[52] E. F. Arruda, S. S. Das, C. M. Dias, D. H. Pastore, *PLOS ONE* **2021**, *16*, 9, e0257512.

[53] A. Azizi, N. L. Komarova, D. Wodarz, *bioRxiv [preprint] Available from:* `https://doi.org/10.1101/2021.09.09.459585` **2021**.

[54] B. F. Nielsen, A. Eilersen, L. Simonsen, K. Sneppen, *Epidemics* **2021**, *40*, 100613.

[55] S. Bugalia, J. P. Tripathi, H. Wang, *arXiv [preprint] Available from:* `https://doi.org/10.48550/arXiv.2201.06285` **2022**.

[56] U. A.-P. de León, E. Avila-Vales, K.-l. Huang, *Chaos Solit. Fractals* **2022**, *157*, 111927.

[57] A. T. Layton, M. Sadria, *Sci. Rep.* **2022**, *12*, 2114.

[58] A. Dutta, *Research Square [preprint] Available from:* `https://doi.org/10.21203/rs.3.rs-1132140/v1` **2021**.

[59] W. M. Getz, R. Salter, L. Luisa Vissat, J. S. Koopman, C. P. Simon, *J. R. Soc. Interface* **2021**, *18*, 184, 20210648.

[60] G. Gonzalez Parra, A. J. Arenas, *SSRN [preprint] Available from:* `https://doi.org/10.2139/ssrn.4119450` **2022**.

[61] SafeGraph Inc., SafeGraph, **2021**, URL `https://www.safegraph.com`, (Accessed: October 2022).

[62] United States Census Bureau, Explore Census Data, `https://data.census.gov/cedsci`, (Accessed: October 2022).

[63] Centers for Disease Control and Prevention, Quarantine and isolation, **2022**, URL `https://www.cdc.gov/coronavirus/2019-ncov/your-health/quarantine-isolation.html`, (Accessed: October 2022).

[64] Covid ActNow, Westchester County, NY, `https://covidactnow.org/us/new_york-ny/county/westchester_county/?s=28041695`, (Accessed: October 2022).

[65] A. A. Sayampanathan, C. S. Heng, P. H. Pin, J. Pang, T. Y. Leong, V. J. Lee, *The Lancet* **2021**, *397*, 10269, 93.

[66] P. Wu, F. Liu, Z. Chang, Y. Lin, M. Ren, C. Zheng, Y. Li, Z. Peng, Y. Qin, J. Yu, et al., *Clinical Infectious Diseases* **2021**, *73*, 6, e1314.

[67] J. M. Dan, J. Mateus, Y. Kato, K. M. Hastie, E. D. Yu, C. E. Faliti, A. Grifoni, S. I. Ramirez, S. Haupt, A. Frazier, et al., *Science* **2021**, *371*, 6529, eabf4063.

[68] COVID-19 Forecast Hub, COVID-19 New York weekly forecast summary, `https://covid19forecasthub.org/reports/single_page.html?state=NY&week=2021-03-30#County_level`, (Accessed: October 2022).

[69] COVID-19 Forecast Hub, COVID-19 Connecticut weekly forecast summary, `https://covid19forecasthub.org/reports/single_page.html?state=CT&week=2021-03-30#County_level`, (Accessed: October 2022).

[70] United States Census Bureau, QuickFacts, Westchester County, New York; United States, `https://www.census.gov/quickfacts/fact/table/westchestercountynewyork,US/PST045219`, (Accessed: October 2022).

[71] Centers for Disease Control and Prevention, COVID data tracker: variant proportions, **2021**, URL `https://covid.cdc.gov/covid-data-tracker/#variant-proportions`, (Accessed: October 2022).

[72] Y. Liu, J. Rocklöv, *J. Travel Med.* **2022**, *29*, 3, taac037.

[73] The official website of New York State, Vaccination progress to date, available at `https://coronavirus.health.ny.gov/vaccination-progress-date`. Accessed: October 2022.

[74] Google, Google News: Coronavirus (COVID-19), **2021**, URL `https://news.google.com/covid19/map?hl=en-US&mid=%2Fm%2F059rby&state=7&gl=US&ceid=US%3Aen`, (Accessed: October 2022).

[75] B. J. Gardner, A. M. Kilpatrick, *MedRxiv [preprint] Available from:* `https://doi.org/10.1101/2021.12.10.21267594` **2021**.

[76] N. Andrews, J. Stowe, F. Kirsebom, S. Toffa, T. Rickeard, E. Gallagher, C. Gower, M. Kall, N. Groves, A.-M. O'Connell, D. Simons, P. B. Blomquist, A. Zaidi, S. Nash, N. Iwani Binti Abdul Aziz, S. Thelwall, G. Dabrera, R. Myers, G. Amirthalingam, S. Gharbia, J. C. Barrett, R. Elson, S. N. Ladhani, N. Ferguson, M. Zambon, C. N. Campbell, K. Brown, S. Hopkins, M. Chand, M. Ramsay, J. Lopez Bernal, *N. Engl. J. Med.* **2022**, *386*, 16, 1532.

[77] T. Patalon, Y. Saciuk, A. Peretz, G. Perez, Y. Lurie, Y. Maor, S. Gazit, *Nat. Comm.* **2022**, *13*, 1.

[78] P. Jüni, S. Baert, A. Corbeil, J. Johnstone, S. N. Patel, P. Bobos, U. Allen, K. A. Barrett, L. L. Barrett, N. S. Bodmer, K. B. Born, L. Bourns, G. A. Evans, J. Hopkins, D. G. Manuel, A. M. Morris, F. Razak, B. Sander, M. Science, R. Steiner, J. Tepper, N. Thampi, A. McGeer, *Science Briefs of the Ontario COVID-19 Science Advisory Table* **2022**, *3*, 56.

[79] Centers for Disease Control and Prevention, CDC COVID-19, **2021**, URL `https://www.cdc.gov/coronavirus/2019-ncov/index.html`, (Accessed: October 2022).

[80] J. M. Dan, J. Mateus, Y. Kato, K. M. Hastie, E. D. Yu, C. E. Faliti, A. Grifoni, S. I. Ramirez, S. Haupt, A. Frazier, C. Nakao, V. Rayaprolu, S. A. Rawlings, B. Peters, F. Krammer, V. Simon, E. O. Saphire, D. M. Smith, D. Weiskopf, A. Sette, S. Crotty, *Science* **2021**, *371*, 6529, eabf4063.

[81] J. Block, *BMJ* **2021**, *374*.

[82] C. Baraniuk, *BMJ* **2021**, *373*.

[83] H. Chemaitelly, H. H. Ayoub, S. AlMukdad, P. Coyle, P. Tang, H. M. Yassine, H. A. Al-Khatib, M. K. Smatti, M. R. Hasan, Z. Al-Kanaani, E. Al-Kuwari, A. Jeremijenko, A. H. Kaleeckal, A. N. Latif, R. M. Shaik, H. F. Abdul-Rahim, G. K. Nasrallah, M. G. Al-Kuwari, A. A. Butt, H. E. Al-Romaihi, M. H. Al-Thani, A. Al-Khal, R. Bertollini, L. J. Abu-Raddad, *Nat. Comm.* **2022**, *13*, 1, 3082.

[84] Reuters, Moderna booster candidate shows strong response against Omicron subvariants, `https://www.reuters.com/business/healthcare-pharmaceuticals/moderna-booster-candidate-produces-strong-antibodies-against-omicron-subvariants-2022-06-22/`, **2022**, (Accessed: October 2022).

[85] Pfizer, Pfizer and BioNTech Announce Omicron-Adapted COVID-19 Vaccine Candidates Demonstrate High Immune Response Against Omicron, `hhttps://www.pfizer.com/news/press-release/press-release-detail/pfizer-and-biontech-announce-omicron-adapted-covid-19`, **2022**, (Accessed: October 2022).

[86] J. P. Townsend, H. B. Hassler, Z. Wang, S. Miura, J. Singh, S. Kumar, N. H. Ruddle, A. P. Galvani, A. Dornburg, *Lancet Microbe* **2021**, *2*, 12, e666.

[87] D. Goldblatt, *Nat. Rev. Immunol.* **2022**, *22*, 6, 333.

[88] M. Stegger, S. M. Edslev, R. N. Sieber, A. C. Ingham, K. L. Ng, M.-H. E. Tang, S. Alexandersen, J. Fonager, R. Legarth, M. Utko, B. Wilkowski, V. Gunalan, M. Bennedbæk, J. Byberg-Grauholm, C. H. Møller, L. E. Christiansen, C. W. Svarrer, K. Ellegaard, S. Baig, T. B. Johannesen, L. Espenhain, R. Skov, A. S. Cohen, N. B. Larsen, K. M. Sørensen, E. D. White, T. Lillebaek, H. Ullum, T. G. Krause, A. Fomsgaard, S. Ethelberg, M. Rasmussen, *medRxiv [preprint] Available from: https://doi.org/10.1101/2022.02.19.22271112* **2022**.

Table of Contents
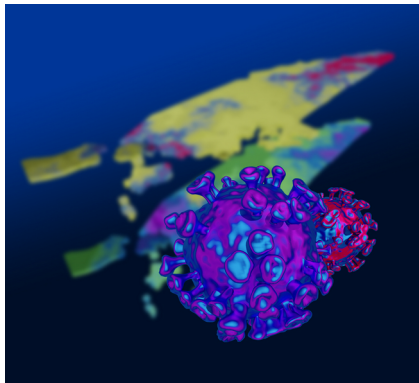
Mathematical models have arisen as powerful tools in the worldwide fight against COVID-19. This paper establishes a high-resolution computational framework for modeling the simultaneous spread of two variants in a medium-size US town. The model is used to study how tests and vaccines can effectively curb new COVID-19 waves and help us prepare for the next phases of this pandemic.